

Helium Atom Scattering/Diffraction

Jason Stotter

4/27/01

CEM 924

Helium Atom Scattering/Diffraction

Introduction	1
Brief History	1
Equipment	1
Elastic Measurements	2
Elastic Mechanism	2
Example Elastic Measurements	2
Inelastic Measurements	3
Inelastic Mechanism	3
Example Inelastic Measurements	3
Elastic/Inelastic Example Measurements	4
He* Measurements	5
Mechanism	5
Example Measurements	5
Summary	5
References	7

Introduction

Brief History

Helium Atom Diffraction was first used in attempts to show the wave character of atoms in the late 1920's by Stern¹. A diffraction of atomic hydrogen from the surface of ice had been claimed by Johnson in 1927, but this was retracted in 1928, with an explanation that erroneous diffraction patterns were an artifact of incorrectly calibrated equipment. In 1929, Stern reported a successful diffraction in his system and recorded the first atom-surface diffraction spectrum.

Stern had chosen to work with He after studying the behavior of several different gas beams interacting with crystal surfaces and achieving diffraction results with only H₂ and Helium. In addition to Helium being a closed-shell, neutral atom that interacts strictly with surfaces, it turns out that He has a nearly perfect mass that allows supersonic beams to have enough energy to interact with surface phonons. Helium also has a smaller size than other closed-shell atoms that allows it to diffract from surfaces by reflecting from peaks and troughs between atoms.

In the late 1960's, experiments by Smight, O'Keefe, Salsburg, and Palmer with Argon and Neon beams on LiF surfaces led to the current understanding of the interaction of Helium atoms' interactions with surfaces¹. Calling the interaction model the "Corrugated Wall Model," these investigators found evidence that gas-surface interactions are due to a strongly repulsive interaction of the electron densities of closed-shell atoms and electron-rich surfaces. In effect, Helium atoms incident on a surface can only near the surface and are then repelled by the surface electrons. If the size of the incident atom is small and light enough, as is Helium, relative to many surfaces studied, it will "see" the surface as a corrugated mirror, the corrugations being the ridges and troughs between individual atoms.

With more work in the area, better sources for molecular beams were developed, allowing workers to direct more mono-energetic beams of Helium atoms at surfaces of interest¹. By directing molecular beams at surface and the measuring

reflected Helium atoms, workers can study both the regular topography of a surface and the mechanics of surface phonons.

Equipment

The Helium atom beam sources used most often produce a supersonic stream of atoms with a very small kinetic energy distribution, with $\Delta V/V$ of about 0.3% possible¹. The He atoms are directed at the sample surface which is mounted so that it can be manipulated relative to the beam. The scattered He atoms follow an arm of an ultrahigh vacuum chamber that is differentially pumped to allow quick removal of atoms that have been skimmed by masks between each stage so that further collisions with other atoms, leading to loss of information and noise, does not occur².

Elastic Scattering/Diffraction

Elastic Mechanism

In elastic methods, a beam of monoenergetic helium atoms is produced incident to a sample surface. The atoms' kinetic energies are small enough and the fields of the incident atoms are large enough that they do not enter the bulk beyond the sample surface, in contrast to even low energy electrons, which enter the first few layers of the bulk. Incident atoms interact with the electron cloud only. An analogy for elastic diffraction is a stream of ping-pong balls aimed at some incident angle at a corrugated steel roof².

The stream of helium atoms is chopped either before it encounters the surface or after the collision on the way to a time of flight mass spectrometer. Short pulses or packets of helium atoms collide with the surface. Most are reflected elastically and continue on to the detector with the same amount of kinetic energy and velocity as when leaving the source.

The reflected atoms are counted either at the specular angle to measure reflectance changes in time, or at varying reflection angles to study surface arrangement of atoms and adatoms. Reflection intensity is often plotted against the angle of reflection for these measurements. The angle of incidence can be varied to change the orientation of surface features to the beam and information about the surface

topography can be gathered by the scattering pattern or diffraction effects. Figure 1 illustrates the Corrugated Hard Wall model of surface diffraction. Azimuthal angle can be changed to map the arrangement of atoms on the surface.

It is impossible to take elastic scattering measurements without also measuring diffraction effects. When a beam of helium atoms is incident to a surface, both elastic and inelastic scattering and diffraction effects are measured. Changing the incident angle and energy allows workers to enhance one effect over another.

Example Elastic Measurements

The atoms that are elastically reflected from the surface at the same angle from surface normal as the incident beam is called the specular beam and intensities of the specular beam may be measured over time, for example, during the growth of a film, to monitor changes in the surface. This type of measurement was presented by Tolkes, Zepenfiled, Krzyzowski, Davies, and Comsa in the study of Cobalt nanostructures in thin films homoepitaxially deposited on a reconstructed gold(111) surface³. Figure 2 shows specular reflectivity curves for deposition at different temperatures. The curves at 100 and 420K show exponential decay of the specular reflectivity as expected for ideal film growth. At 300K, the curve shows maxima and minima corresponding to a growth pattern that deviates from the ideal layer-by-layer mechanism.

Elastic scattering and diffraction measurements are often complimentary, as in Pating, Farias, and Rieder's measurements of Rh(311) step-edge orientations⁴. Figure 3 shows a typical elastic scattering plot of reflection intensity versus angle, here, the incident angle plus the measured angle from surface normal. This plot shows two curves, one for a smooth as-cut surface, and a lighter plot for a sputtered surface with numerous defects. Note that the widths of the peaks for the sputtered surface are wider because of reflection and diffraction from surface defects. Each of these peaks was attributed to a facet on the stepped surface. To assign peaks to specific surface features, the same measurement was taken at varying angles of incidence. These results are shown in figure 4, where peaks appear and disappear with varying angles of

incidence. Peaks that remain through all angles of incidence tested are attributed to scattering effects, and those that move or disappear through various angles of incidence are attributed to diffraction effects.

Elastic scattering/diffraction may also be used to map a surface in two dimensions by collecting these spectra at varying azimuthal angles and compiling them into two-dimensional plots of surface scattering/diffraction. This method was used by Glebov, Graham, Menzel, and Toennies in a study of the surface of an ice crystal grown on a Pt(111) surface⁵. Figure 5 shows the intensity of scattered atoms measured at varying polar angles with very low-energy incident atoms. This incident energy of 10.5meV and low temperature of 45K was chosen for these experiments because they reduced the incidence of inelastic interactions with the surface. The specular scattering peak (00) and first order diffraction peaks (10) and ($\bar{1}0$) can be seen clearly in one of the two azimuths measured, and not in the other. Figure 6 shows a 2-dimensional map of the arrangement of surface scattering/diffraction created from angular distribution measurements made at 61 different azimuthal angles. From the diffraction pattern it can be calculated that the arrangement of molecules at the surface of this ice crystal is hexagonal and the lattice constant is 4.52 Å.

Inelastic Methods

Inelastic Mechanism

The real strength of Helium atom beam methods lies in the measurement of surface phonons. Lattice vibrations of solids are excited to resonant vibrational band modes called phonons. Phonons may exist at the surface of a solid as either the surface termination of a bulk phonon, or a surface-specific vibrational mode². Helium atoms move slowly enough and can be directed at a surface with the correct amount of energy to excite or destroy surface phonons¹¹. The measurement of the loss or gain of energy of these beams from inelastic scattering and diffraction has allowed workers to study phonon mechanics for many crystals. Workers enhance inelastic phonon-interaction over elastic scattering by varying the amount of energy available for transfer

normal to the surface by varying the incident angle, and by adjusting the kinetic energy of the atoms released from the source.

Figure 7 provides a schematic for inelastic interactions. If the relative intensities at varying angles from the specular beam are measured, phonon modes may be interpreted as maxima. Phonon annihilation requires energy transfer from the surface, so atoms are reflected closer to normal. Phonon creation requires energy transfer to the surface, so atoms are reflected further from surface normal⁶. The atomic beam is chopped into pulses of incident atoms and atoms from all reflection angles are collected and counted with a time of flight mass spectrometer. With a relatively mono-energetic atomic beam, counts of atoms from each pulse that arrive at the detector before or after the specular atoms may be converted to energy loss spectra for the interaction with the surface.

Example Inelastic Measurements

In a study of ultrathin Barium films on the Cu(100) surface, Bartholmei et al. present such energy transfer plots⁷. Figure 8 shows energy loss spectra for a bare Cu(100) surface and the same surface with 1, 2, and 3 monolayers of Ba coverage. The beam incident and azimuthal angles were the same in all experiments, as was the surface temperature. The plot for the bare surface shows the specular beam and the single Rayleigh phonon, a translational phonon characteristic of metal single crystals. This phonon is not accessed by the helium atoms when even one monolayer of Ba covers the surface because of the large acoustical impedance difference between the metal crystal and the barium film. The first order surface phonons for the surface covered with barium, which do not appear on the spectrum for the clean copper surface, decrease logarithmically in energy transfer with increasing coverage, confirming for the authors a step-flow growth model.

Example Elastic/Inelastic Measurements

The suite of Helium beam methods are most often used as one of several tools used to learn about a system. Helium atom methods can often provide insight to make more clear the interpretation of results from other methods. A good example is the

use of elastic scattering/diffraction, inelastic scattering, and LEED measurements by Graham and Toennies in the study of structures formed by Sodium on Copper (001) in submonolayer amounts⁸. The study was completed at low temperatures to limit the diffusion of the otherwise mobile sodium atoms across the surface.

The first measurements presented are specular reflectivity measurements, where specular reflectivity is defined as the ratio of the intensity of the elastic specular beam of a partially covered surface to that of a clean, uncovered surface. Figure 9 shows the specular reflectivity for the surface plotted against a fraction of surface coverage at a constant surface temperature of 40K. Specular reflectivity maxima on these plots, after comparison with LEED results, were attributed to ordered surface structures which more coherently reflected and diffracted incident atoms than disordered structures.

Time of flight mass spectra for inelastic measurements are also presented for increasing fractional coverages of sodium on the metal surface in figure 10. At each coverage, a large elastic peak is observed, as well as several inelastic peaks that change frequency with increasing coverage. As an example of the power of coupling HAD and LEED measurements, note the frequency shift of the ± 6 eV peak to a ± 2 eV peak with coverage increasing past 0.2. Two possible explanations for this shift are given by the authors. One explanation is a change in the Na binding site from a 4-fold hollow to an on-top site. However, LEED patterns show no change in binding arrangement at these levels of coverage. The more likely explanation is due to a change in Na to Na neighbor interactions within a layer while remaining in the 4-fold hollow binding sites. This change in interactions is attributed to metallization of the bonding of Na and other alkali metals to metal single crystal surfaces, reducing the interaction of neighboring alkali metal atoms.

He* Measurements

He* Mechanism

The change in the electron density of states of metal single crystal surfaces with the addition of alkali metals mentioned above has been exploited recently in a new

application of molecular beam methods. One more layer of surface specificity has been added to the application of helium atom beams. Fouquet and Witte presented a variation of helium atom scattering in which metastable excited helium atoms are used as the incident particles⁹. These excited helium atoms relax to their ground state upon interaction with the surface as a function of the surface density of states. One application of this effect is the study of the electronic effects of alkali metal adsorption on metal single crystals. The adsorption of the alkali metals on the single crystal surface changes the surface density of states interaction with the excited atoms so that their probability of interacting with the surface without relaxing has been shown to be decreased by as much as 100-fold.

Example He* Measurements

In a study of poisoning of alkali metal films by O₂ and CO₂ adsorption by Fouquet and Witte, reflected He and He* atoms were collected and differentially counted by mass spectrometer and magnetron¹⁰. These intensities as the films were poisoned by O₂ and CO₂ were compared to find the increasing survival of He* as the surface was demetallized by adsorbed molecules. Figure 11 shows the difference in He* survival with O₂ dosage for a clean Cu(100) surface to those with one monolayer of adsorbed Na, K, and Cs.

Summary

Since their first use nearly seventy years ago in the verification of quantum-mechanical ideas about matter, helium atom methods have only seen active application in the last thirty years due to development of suitable vacuum equipment, mass spectrometers, and supersonic nozzle atomic beam sources. Of all molecular and atomic beam methods, helium atom scattering and diffraction have found the most utility in studying surfaces, especially surface phonons, owing to helium's size and mass, and worker's ability to create mono-energetic helium beam sources. Elastic and inelastic collisions provide non-destructive way to probe the surface for both topographical features and phonon modes.

These methods are very often used in a study alongside LEED measurements. Where LEED is very good at presenting the arrangement of electron cores in the bulk near a surface, Helium Atom methods only interact with the very surface of the material. Pairing complementary data gives a clearer picture of the surface than either method alone.

It seems that only workers interested in surface phonons find use for any of the helium atom beam methods. This is probably because, for other applications such as measuring surface coverage of adlayers, there exist better, simpler methods. Helium atom scattering, for example, is only used for measuring surface coverage when workers have constructed a vacuum system containing the necessary apparatus as part of a phonon study. However, these methods will likely see wider use in coming years as the study of alkali metals on surfaces with beams of excited helium atoms becomes more common.

References

1. Valbusa, U.; General Principles and Methods. In *Atomic and Molecular Beam Methods*; Laine, D., Valbusa, U., Eds.; Oxford University Press: New York, 1992; 2, pp 327-339.
2. Benedek, G., Toennies, J.; Helium atom scattering spectroscopy of surface phonons: genesis and achievements. *Surf. Sci* **1994**, *299*, pp 587-611.
3. Tolkes, C., Zeppenfeld, P., Krzyzowski, M. A., Davis, R., Comsa, G.; Growth and stability of cobalt nanostructures on gold (111). *Surf. Sci.* **1997**, *394*, pp 170-184.
4. Patting, M., Farias, D., Rieder, K. H.; Determination of step-edge orientation by helium atom scattering. *Phys. Rev. B.* **2000**, *62*, pp 2108-2112.
5. Glebov, A., Graham, A. P., Menzel, A., and Toennies, J. P.; A helium atom scattering study of the structure and phonon dynamics of the ice surface. *J. Chem. Phys.* **2000**, *112*, pp 11011-11022.
6. Woodruff, D. P., Delchar, T. A.; Atomic and Molecular Beam Scattering. *Modern Techniques of Surface Science*, 2nd ed.; Cambridge University Press: New York, **1994**; pp 485-531.
7. Bartholmei, S., Fouquet, P., Witte, G. Growth and dynamics of ultrathin barium films on Cu(100). *Surf. Sci.* **2001**, *473*, pp 227-235.
8. Graham, A. P., Toennies, J. P.; Helium-atom diffraction study of the submonolayer structures of sodium on Cu(001). *Phys. Rev. B.* **1997**, *56*, pp 15378-1590.
9. Fouquet, P., Witte, G.; Observation of Metallization Transition of 2D Alkali Metal Films. *Phys. Rev. Lett.* **1999**, *83*, pp 360-363.
10. Fouquet, P., Witte, G.; Monitoring of electronic poisoning of ultrathin alkali metal films by oxygen and carbon monoxide adsorption. *Surf. Sci.* **2000**, *454-456*, pp 256-251.
11. Doak, R. B.; Single-Phonon Inelastic Helium Scattering. In *Atomic and Molecular Beam Methods*; Laine, D., Valbusa, U., Eds.; Oxford University Press: New York, 1992; 2, pp 385-443.

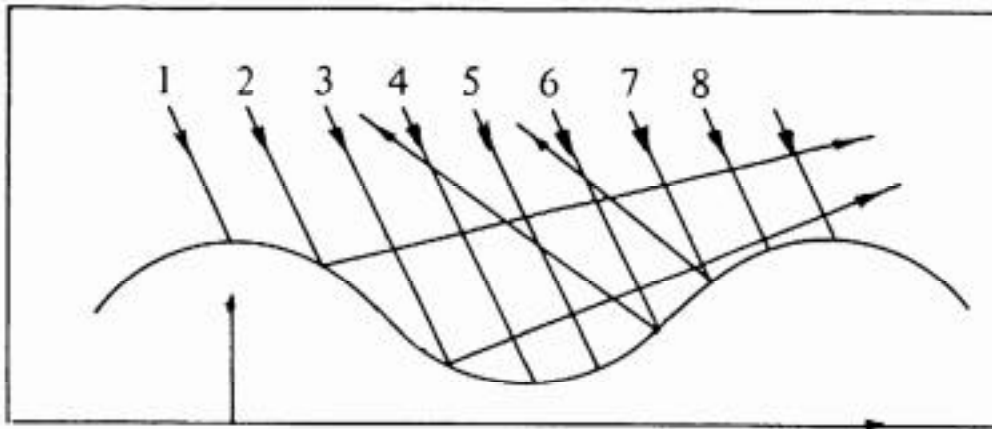


Figure 1. Illustration of rainbow diffraction of particles travelling in parallel direction by a corrugated surface. From Woodruff, D. P., Delchar, T. A.; Atomic and Molecular Beam Scattering, *Modern Techniques of Surface Science*, 2nd ed.; Cambridge University Press: New York, 1994; pp 485-531.

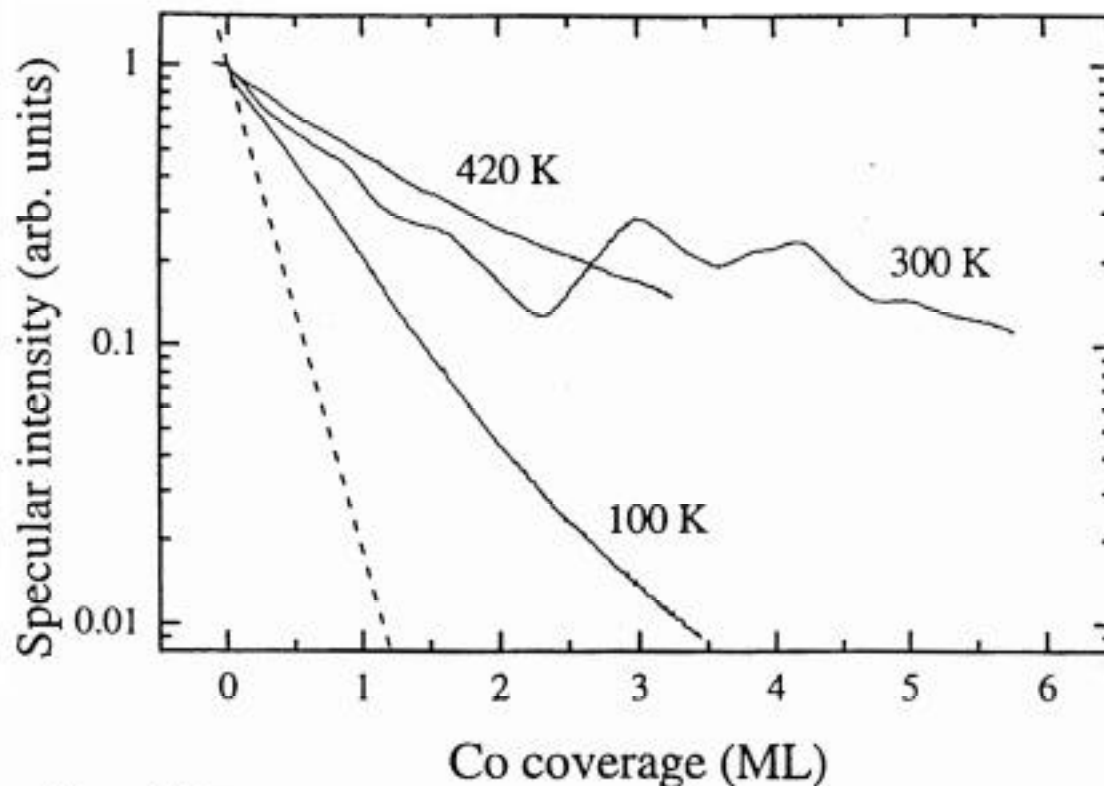


Figure 2. Helium specular reflectance deposition curves for various surface temperatures compared. From Tolkes, C., Zeppenfeld, P., Krzyzowski, M. A., Davis, R., Comsa, G.; Growth and stability of cobalt nanostructures on gold (111). *Surf. Sci.* 1997, 394, pp 170-184.

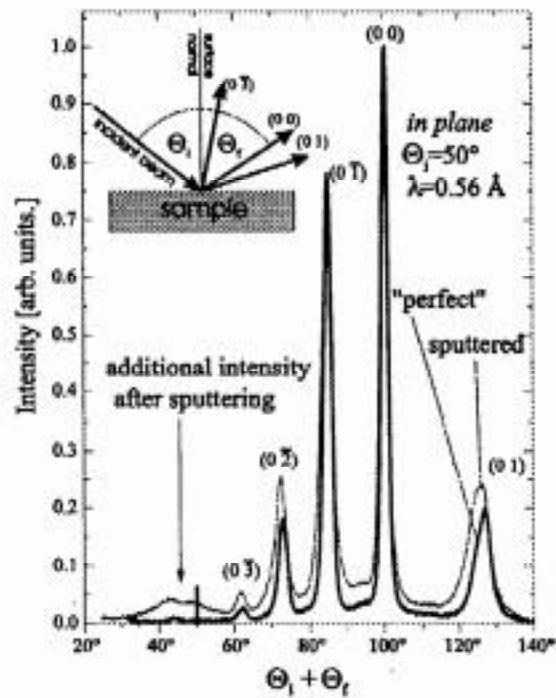


Figure 3. Elastic intensity versus angle (incident plus measured angle) for as-cut and sputtered Rh (311) surface. From Patting, M., Farias, D., Rieder, K. H.; Determination of step-edge orientation by helium atom scattering. *Phys. Rev. B.* 2000, 62, pp 2108-2112.

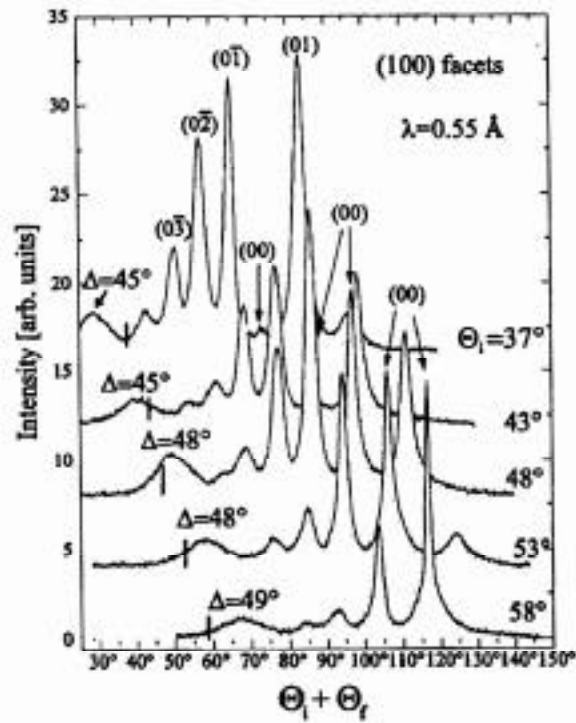


Figure 4. Elastic intensity versus angle (incident plus measured angle) for changing incident angles. From Patting, M., Farias, D., Rieder, K. H.; Determination of step-edge orientation by helium atom scattering. *Phys. Rev. B.* 2000, 62, pp 2108-2112.

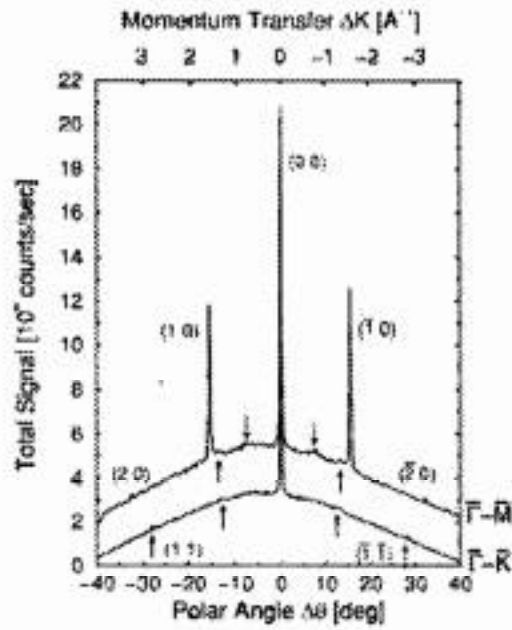


Figure 5. Angular distribution of inelastic intensity along two azimuths of an ice Ih surface. From Glebov, A., Graham, A. P., Menzel, A., and Toennies, J. P.; A helium atom scattering study of the structure and phonon dynamics of the ice surface. *J. Chem. Phys.* 2000, 112, pp 11011-11022.

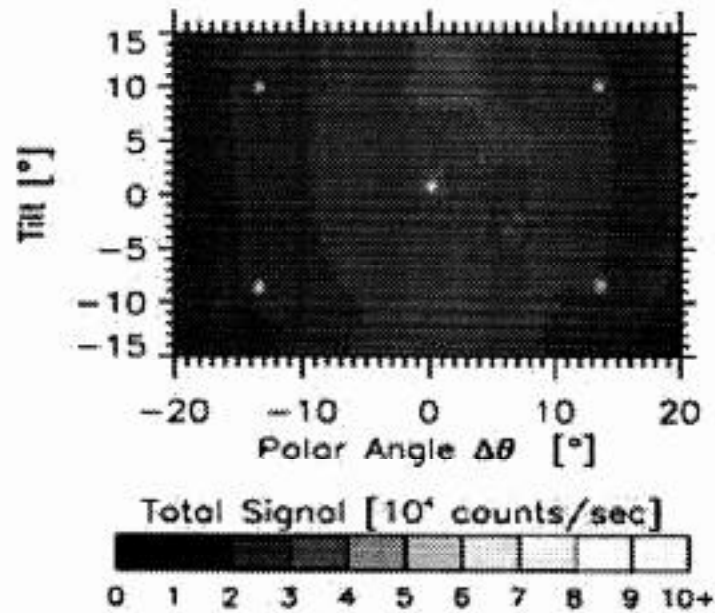


Figure 6. Two-dimensional plot of diffraction intensities from measurements at 61 azimuthal angles of an ice Ih surface. From Glebov, A., Graham, A. P., Menzel, A., and Toennies, J. P.; A helium atom scattering study of the structure and phonon dynamics of the ice surface. *J. Chem. Phys.* 2000, 112, pp 11011-11022.

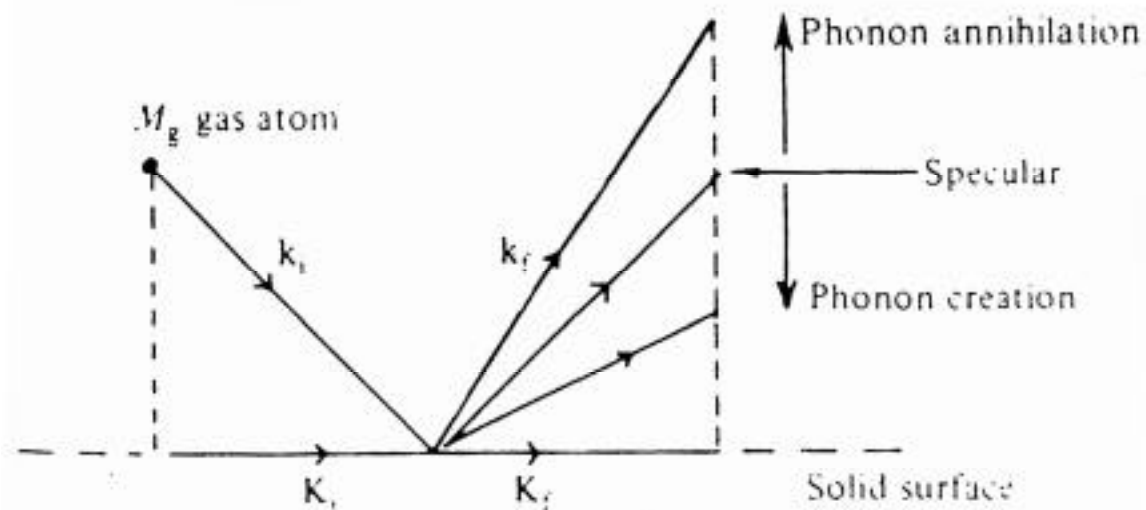


Figure 7. Schematic of inelastic scattering. From Woodruff, D. P., Delchar, T. A.; Atomic and Molecular Beam Scattering. *Modern Techniques of Surface Science*, 2nd ed.; Cambridge University Press: New York, 1994; pp 485-531.

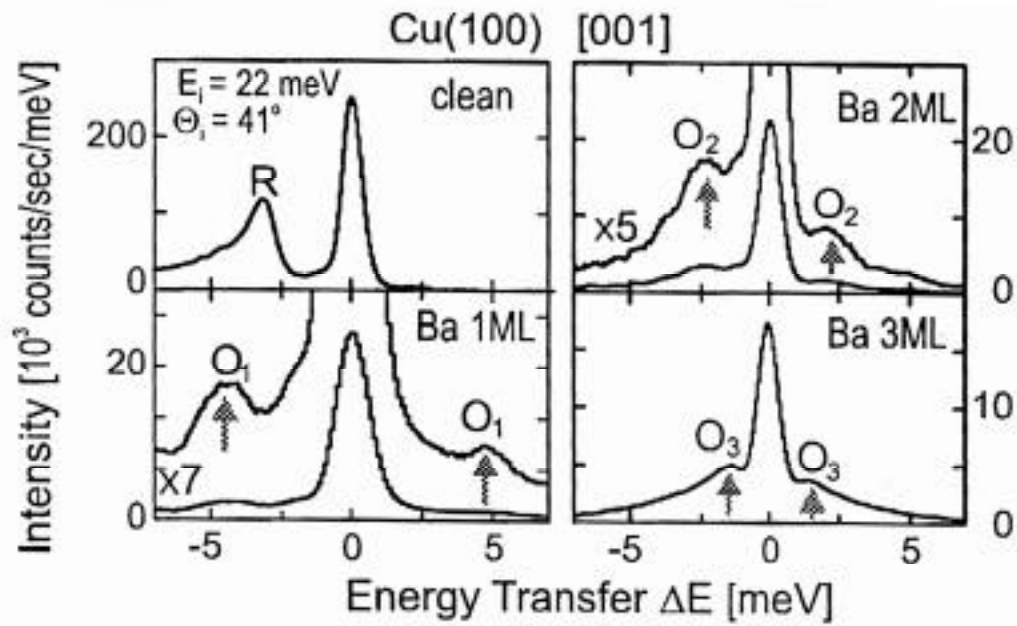


Figure 8. Energy loss spectra for inelastic scattering from Cu (100) with 0, 1, 2, and 3ML Ba coverage. From Bartholmei, S., Fouguet, P., Witte, G. Growth and dynamics of ultrathin barium films on Cu(100). Surf. Sci 2001, 473, pp 227-235.

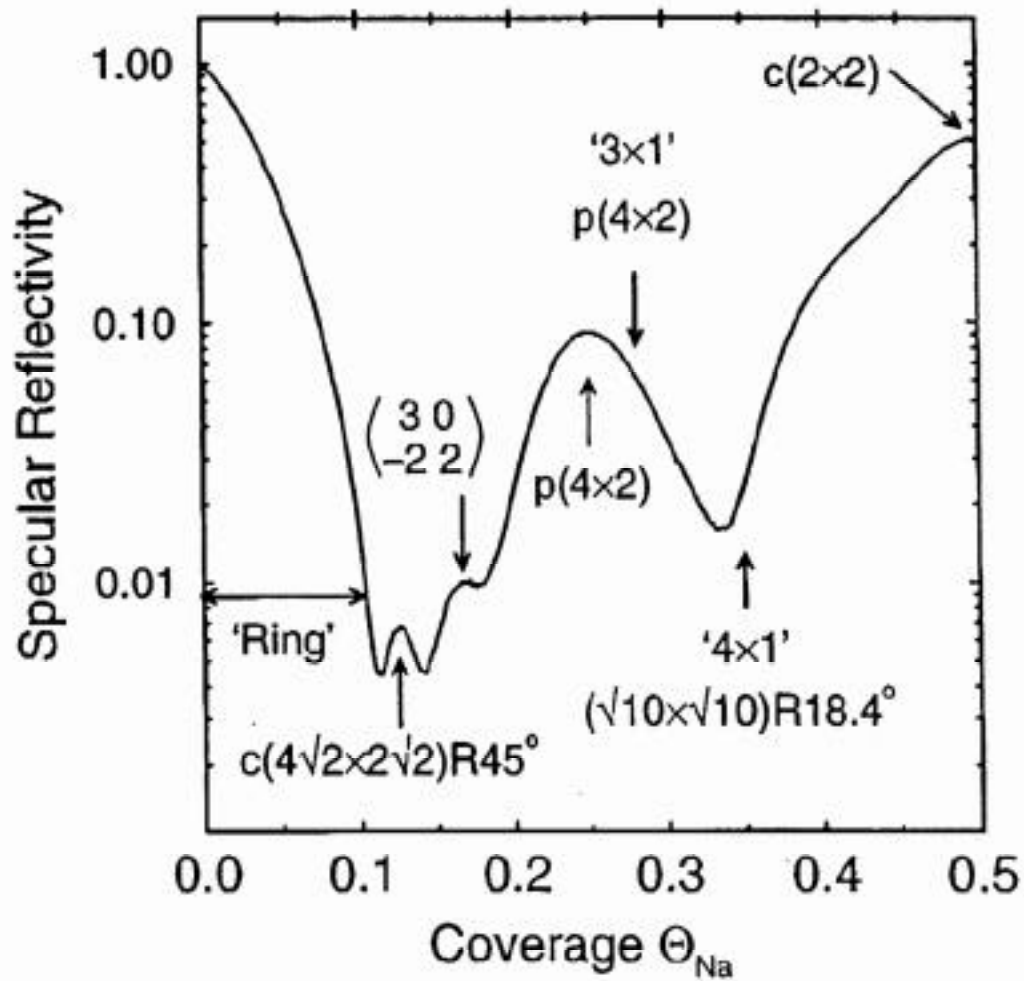


Figure 9. Specular reflectivity versus fractional coverage of Na on Cu(100). From Graham, A. P., Toennies, J. P.; Helium-atom diffraction study of the submonolayer structures of sodium on Cu(001). *Phys. Rev. B.* 1997, 56, pp 15378-1590.

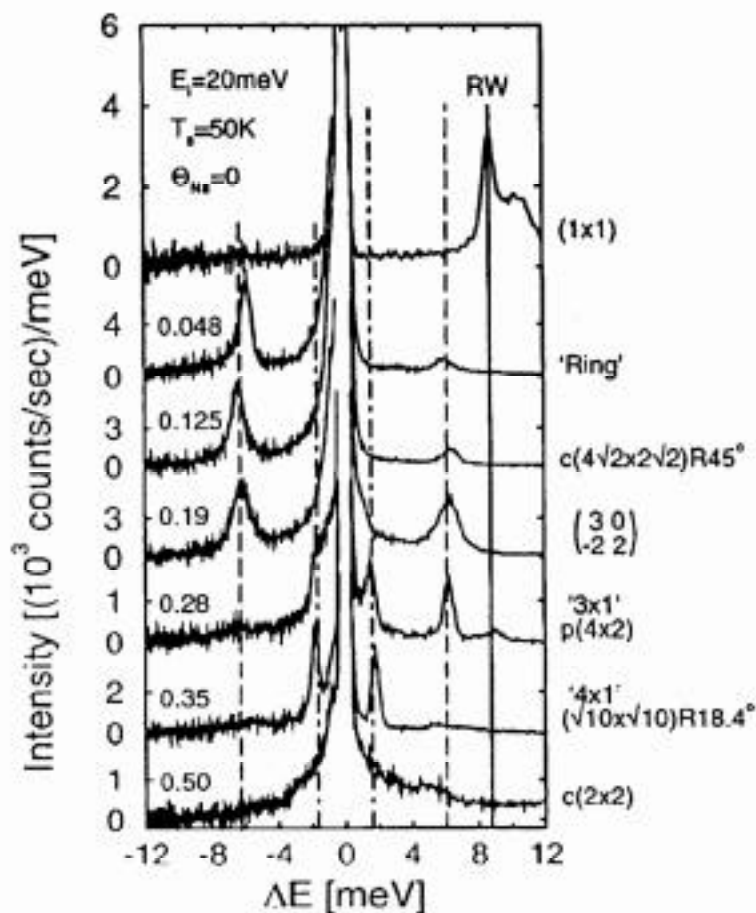


Figure 10. Energy loss spectra for varying fractional coverage of Na on Cu(100).
 From Graham, A. P., Toennies, J. P.; Helium-atom diffraction study of the submonolayer structures of sodium on Cu(001). *Phys. Rev. B.* 1997, 56, pp 15378-1590.

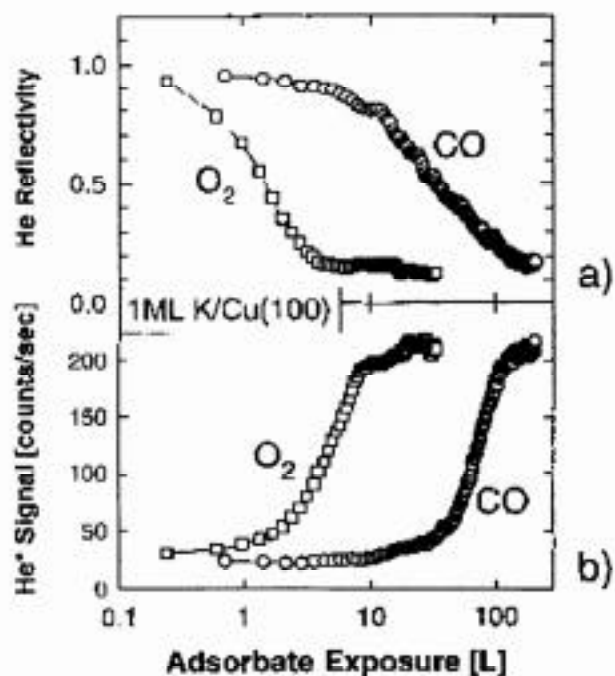


Figure 11. Scattered He* versus O₂ exposure for a clean Cu (100) surface and Cu (100) surface covered with 1ML of Cs, K, and Na. From Fouquet, P., Witte, G.; Monitoring of electronic poisoning of ultrathin alkali metal films by oxygen and carbon monoxide adsorption. *Sur. Sci.* 2000, 454-456, pp 256-251.